Ferromagnetism, superconductivity and quantum criticality in uranium intermetallics

Nguyen Thanh, H.

Publication date
2008

3. Theoretical aspects

3.1. Fermi liquid and non-Fermi liquid behavior

3.1.1. Fermi liquid behavior

Heavy fermion systems (HFSs) are mainly found among intermetallic compounds, which contain a rare-earth or actinide atom (*i.e.* Ce, Yb and U) with a partially filled *f*-electron shell. At high temperatures, the conduction electrons are decoupled from the *f*-electrons, which behave as localized moments. At low temperatures, the *f*-electrons strongly couple to the conduction band and delocalize which results in an enhancement of the effective mass m^* to values 100 - 1000 times larger than the bare electron mass m_e. The crossover temperature between the localized and delocalized regime is the coherence temperature T_{coh}. A valid description of HFSs is provided by the notion of quasiparticles, as in Landau's Fermi liquid (FL) theory [5,58]. However, the use of the FL theory is restricted to a temperature range $T < T_{coh}$, where T_{coh} is typically inversely proportional to the effective mass enhancement, thus can be much smaller than the Fermi temperature T_{FL}.

Landau's theory is used to describe interacting systems or Fermi liquids, with particles (electrons) that have spin ½ excitations and obey Fermi - Dirac statistics. Because of the interaction between electrons, an electron collects around itself a screening cloud of surrounding electrons. These are considered as independent entities so-called quasiparticles with an effective mass m^*. At low temperatures, much below a characteristic (Fermi) temperature T_{FL}, the system behaves almost the same way as a non-interacting Fermi gas. The main assumption in the FL model is that, as the interaction is adiabatically turned on, there exists a one-to-one correspondence between the low energy eigenstates of the

interacting system and the single-particle states of the Fermi gas. Therefore, the interacting Fermi liquid exhibits similar thermodynamic properties as the non-interacting Fermi gas, *e.g*. a linear T dependence of the specific heat $c = \gamma T$ and a constant Pauli paramagnetic susceptibility χ_0. However, the enhancement of the effective mass in the Fermi liquid leads to enhanced values of these coefficients.

At low T, the quasiparticle scattering rate quadratically depends on temperature as $1/\tau \sim T^2$, with τ the quasiparticle lifetime. This leads to a quadratic temperature dependence of the electrical resistivity $\rho(T)$ at low temperatures. In the $T \rightarrow 0$ limit, the resistivity becomes constant and is determined by lattice imperfections and intrinsic impurities. Thus the electrical resistivity can be expressed by

$$\rho(T) = \rho_0 + AT^2 \qquad (3.1)$$

where ρ_0 is the residual resistivity.

In heavy fermion systems, there is a universal relation between the coefficient A and the coefficient of the electronic specific heat γ, as presented by the empirical Kadowaki - Woods ratio $A/\gamma^2 = 10\ \mu\Omega\text{cmK}^2\text{mol}^2\text{J}^{-2}$ [59].

In the most simple model, below a certain temperature, T_K, the *f*-electron HFS forms a new electronic state, with an enhanced effective mass, due to the exchange interaction between localized and conduction electrons. This phenomenon is well known as the Kondo effect [31], which is often used to discuss the interaction of an isolated magnetic impurity with the conduction electrons in non-magnetic metals. Here T_K is the Kondo temperature. HFSs in which local spins of the magnetic impurities interacting with conduction electrons build up a regular periodic lattice are known as Kondo lattices and are described by Doniach's model [28].

This model describes a one-dimensional "lattice", the "Kondo necklace" with Hamiltonian

$$H = H_K + H_{RKKY} \qquad (3.2)$$

where H_K is the Kondo Hamiltonian and H_{RKKY} is due to the Ruderman-Kittel-Kasuya-Yosida (RKKY) interaction.

H_K describes the exchange of the local impurity spin (S) with a conduction electron spin (σ)

$$H_K = -2J\boldsymbol{S}.\boldsymbol{\sigma} \qquad (3.3)$$

The exchange parameter J is negative which represents antiferromagnetic coupling of

the magnetic impurity spin to the conduction electron spin. In the ground state, the impurity spin is completely compensated by the surrounding electron spins. This indicates the system tends to a non-magnetic ground state or Kondo singlet, which leads to the formation of a narrow peak in the density of state close to the Fermi level, the so-called Kondo resonance. The binding energy of the Kondo singlet in the weak coupling regime is

$$k_B T_K = \frac{1}{N(0)} e^{-1/JN(0)} \qquad (3.4)$$

where T_K is the characteristic Kondo temperature, which is typically of the order 10 - 100 K and approximately corresponds to the coherence temperature T_{coh}.

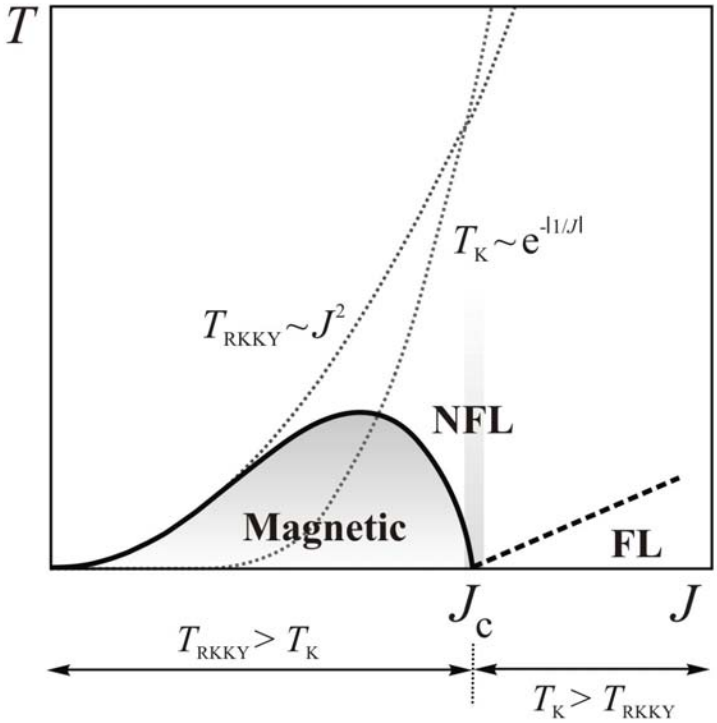

Figure 3.1 Doniach phase diagram (FL and NFL stand for Fermi liquid and non- Fermi liquid, respectively). The dotted lines represent T_K and T_{RKKY}. The full line indicates the magnetic ordering temperature. The dashed line represents the characteristic temperature T_{FL} below which FL behavior is attained.

H_{RKKY} presents the effect of the "long-range" coupling between the local spins, which can be due to the direct exchange between *f*-orbitals or mediated by the polarization of the conduction electrons, H_{RKKY} can gives rise to magnetic order.

$$H_{RKKY} = \sum_{i,j} I_{ij} \sigma_i \sigma_j \qquad (3.5)$$

where I_{ij} = N(0) J^2 $F(k_F R_{ij})$ with R_{ij} the distance between the lattice sites *i*, *j* and $F(x) \equiv F(k_F R_{ij}) = (x\cos x - \sin x)/x^4$ is the oscillating term. $F(x)$ may be positive or negative,

and, therefore, the system can be ferro- or antiferromagnetic, respectively. The energy associated with the RKKY interaction is

$$k_B T_{RKKY} = N(0)\, C\, J^2 \qquad (3.6)$$

where C is a dimensionless constant which depends on the band structure.

Within Doniach's analysis, the ground state of the Kondo lattice system is a consequence of the competition between the Kondo effect and the RKKY interaction [30], as represented in Fig. 3.1. Notice that both interactions depend on the same exchange parameter J.

For small J, $T_{RKKY} > T_K$ and the system orders magnetically. With J increasing, the Kondo effect gradually becomes stronger and magnetism becomes weaker. At a critical value J_c where $T_{RKKY} = T_K$ a second-order transition from a magnetic to a non-magnetic phase is observed, thus the system at $J = J_c$ has a magnetic instability. For $J > J_c$, the Kondo effect prevails as $T_K > T_{RKKY}$, and the system has a non-magnetic ground state.

3.1.2. Non-Fermi liquid behavior

As mentioned above, the FL theory is useful to explain the low-temperature properties of many intermetallic compounds. However, in the past decade, experiments demonstrated that there are a number of HFSs [60-62] with physical properties that significantly deviate at low temperatures from the predictions of the FL theory, the so-called non-Fermi liquid (NFL) systems. NFL behavior in *f*-electron systems is often characterized by weak power law or logarithmic temperature dependences of the thermodynamic and transport properties at low temperatures $T < T_{coh}$. The specific heat $c(T)/T$ diverges logarithmically for $T \rightarrow 0$, the magnetic susceptibility $\chi(T)$ varies as $1 - T^{1/2}$ or $-\ln T$ or T^{-m} ($m \approx \frac{1}{3}$), and the electrical resistivity shows a non-quadratic temperature dependence $\rho(T) \sim T^n$ with $n < 2$. The unusual NFL temperature dependences are observed in doped heavy fermion compounds [17,60-62] as well as in stoichiometric *f*-electron compounds [18,19,33,63]. Up to now, there is no theoretical model, which entirely explains the physics of NFL systems. Nevertheless, several scenarios have been proposed as a route to NFL behavior in *f*-electron materials as described below.

The two-channel Kondo model

In this model [64,65], M degenerate channels of conduction electrons couple, with identical exchange integrals, to a spin-S_I impurity. When $M > 2S_I$, the impurity spin is overscreened

by the spins of the conduction electrons. Subsequently, a non-trivial non-Fermi-liquid critical point governs the low-temperature properties of the system. It has been suggested [66] that this model is based on single-ion physics and may be predominantly observed in U-based compounds with $M = 2$, $S_I = ½$ such as $Y_{1-x}U_xPd_3$ [62], $Th_{1-x}U_xRu_2Si_2$ [67] or $Ce_{1-x}La_xCu_{2.2}Si_2$ [68]. The thermodynamic and transport properties are predicted to vary with temperature as:

$$c(T)/T \sim -\ln T \qquad (3.7a)$$

$$\chi(T) \sim -\ln T \qquad (3.7b)$$

$$\rho(T) \sim -T^{1/2} \qquad (3.7c)$$

Distribution of Kondo temperatures (referred to as the *Kondo disorder model*)

If materials are highly disordered, a distribution of Kondo temperature scales can be generated [69]. Each scale determines the temperature at which Fermi-liquid behaviour will set in around a single magnetic impurity antiferromagnetically coupled to the conduction electrons (assuming an effective spin ½ impurity magnetic moment). Averaging over such a distribution can produce thermodynamic and transport properties which look non-Fermi-liquid, like due to the broad range of effective Fermi temperatures [69,70]. Essentially, the unquenched moments contribute the NFL physics. Similar to th*e two-channel Kondo model*, the Kondo disorder relies on single-ion dynamics and is realized in doped compounds, *e.g.* $UCu_{5-x}Pd_x$ [61]. The temperature variation of the thermodynamic and transport properties is as below

$$c(T)/T \sim -\ln T \qquad (3.8a)$$

$$\chi(T) \sim -\ln T \qquad (3.8b)$$

$$\rho(T) \sim -T \qquad (3.8c)$$

Proximity to a quantum critical point

In the Doniach phase diagram [28], (see Fig. 3.1), with J increasing at zero temperature, the system moves to the right from magnetic to non-magnetic and passes the critical value J_c. At this value the system shows a magnetic instability driven by quantum fluctuations, and J_c is called the quantum critical point (QCP). In HFSs, the QCP can be tuned by changing chemical composition, applying magnetic field or pressure. In the vicinity of the QCP, spin fluctuations are strongly enhanced. This gives rise to NFL temperature dependencies of the thermal and transport properties as follows:

$$c(T)/T \sim -\ln T \qquad (3.9a)$$

$$\chi(T) \sim T^{-m} \quad (m < 1) \qquad (3.9b)$$

$$\rho(T) \sim T^{n} \ (n < 2) \qquad (3.9c)$$

Some theoretical aspects of QCP physics will be presented in more detail in Section 3.2.

Griffiths phase model

In this model developed by Castro Neto [71], the NFL behavior is caused by the competition of RKKY interactions and the Kondo effect in the presence of disorder and magnetic anisotropy.

The theory proposed [71] that in *f*-electron systems the presence of disorder leads to the coexistence of a metallic paramagnetic phase with a granular magnetic phase which is equivalent to the Griffiths phase of dilute magnetic systems [72]. The disordered Kondo lattice problem is mapped onto the random Ising model in a random transverse magnetic field where the disorder is correlated. The result is the coexistence of two electron fluids: one is the paramagnetic metallic phase quenched by the Kondo effect and the other is the granular or spin cluster magnetic phase dominated by the RKKY interactions. At low T, rare strongly coupled magnetic clusters can be considered as giant spins, which can quantum-mechanically tunnel over classically forbidden regions. The thermodynamic properties are predicted to follow the power-law behavior:

$$c(T)/T \sim T^{-1+\lambda} \qquad (3.10a)$$

$$\chi(T) \sim T^{-1+\lambda} \qquad (3.10b)$$

with a nonuniversal positive exponent $\lambda < 1$ (experimentally, $0.7 \leq \lambda \leq 1$).

3.2. Quantum phase transitions

3.2.1. Classical versus quantum phase transitions

Commonly, phase transitions occur at finite temperatures, *e.g.* ice (the solid phase of water) melts and forms a new phase of water, the liquid phase, near 0 ^{o}C; or iron which transforms from magnetic to non-magnetic order at 770 ^{o}C. These are so-called thermal or classical transitions driven by thermal fluctuations characterized by the thermal energy scale $k_{B}T$. Thus temperature is considered as the control parameter for classical phase transitions.

Recently, a different class of phase transitions has attracted a lot of attention. These are

quantum phase transitions (QPTs) which are continuous phase transitions occurring at absolute zero temperature as a function of a non-thermal control parameter, like pressure, chemical doping, magnetic field or electron density. QPTs can be induced in a wide range of materials, such as correlated metals [73], cuprate superconductors [74], common metals [75], and the two-dimensional electron gas [76]. By changing the control parameter, systems can be tuned to the transition point, the so-called quantum critical point (QCP) at which quantum fluctuations characterized by their quantum energy scale $\hbar\omega_c$ dominate rather than thermal fluctuations. Near the QCP, the material exhibits unusual properties, which require novel concepts and theories to describe the singular behavior that have no analogues in their classical counterparts.

A continuous phase transition can be characterized by an order parameter, a concept first introduced by Landau. An order parameter is a thermodynamic quantity that is zero in the disordered phase, and non-zero in the ordered phase, *e.g.* the total magnetization M is chosen for a ferromagnetic transition. When approaching the transition point or the critical point, the spatial correlations of the order parameter become long-ranged. Notably, close to the critical point, the correlation length diverges, like a power law

$$\xi \propto t^{-\nu} \qquad (3.11)$$

where ν is the correlation length critical exponent, and t denotes some dimensionless distance in parameter space from the critical point.

Apart from these long-ranged correlations in space, there are similar effects in the correlation time τ_c, which is the time scale for the system to return to equilibrium after it has been disturbed, as below

$$\tau_c \propto \xi^z \propto t^{-\nu z} \qquad (3.12)$$

where z is the dynamical critical exponent.

The inverse of τ_c defines a critical frequency scale ω_c that goes to zero as criticality is approached, this phenomenon is called critical slowing down

$$\omega_c(t \to 0) \propto 1/\tau_c \to 0 \qquad (3.13)$$

In the case of a classical phase transition that occurs at a non-zero critical temperature T_C, $k_B T > \hbar\omega_c$ and t can be defined as $t = |T - T_C|/T_C$. Consider, within classical statistical mechanics, a Hamiltonian

$$H(p,q) = K(p) + U(q) \qquad (3.14)$$

where p and q are the generalized momenta and positions, and K and U are kinetic and potential energy, respectively. The partition function is

$$Z = \int dp\ dq\ e^{-H/k_BT} = \int dp\ e^{-K/k_BT} \int dq\ e^{-U/k_BT} \qquad (3.15)$$

From this partition function it follows that the system's static properties can be study independently from its dynamical ones or z is independent from all other critical exponents. Therefore "statics and dynamics decouple". The static critical behavior can be study by means of an effective functional of a time-independent order parameter, which is often obtained in d dimensions.

Close to the critical point, the free energy $f = -(1/V)\ k_BT\ \ln Z$ obeys a generalized homogeneity relation which was obtained within the framework of the Renormalization Group (RG) theory [77]

$$f(t, B) = b^{-d} f(tb^{1/\nu}, Bb^{x_B}) \qquad (3.16)$$

where V is the system volume, B is the field conjugate to the order parameter (for a ferromagnet B is the magnetic field), b is a scaling parameter that is an arbitrary positive real number, and $x_B > 0$ is a critical exponent. The homogeneity relation, Eq. 3.16, can be applied for other thermodynamic quantities because all of them can be deduced from the free energy.

In the case of a QPT which occurs at $T = 0$ as a function of a non-thermal control parameter r, $\hbar\omega_c > k_BT$, and t therefore is defined as $t = |r - r_c|/r_c$. Consequently, the typical frequency scale ω_c goes to zero as

$$\hbar\omega_c \propto |t|^{\nu z} \qquad (3.17)$$

In quantum statistics, the partition function of the system is presented as

$$Z = Tr\ e^{-H/k_BT} \qquad (3.18)$$

In contrast to the classical case, "statics and dynamics are coupled". The dynamic critical exponent z needs to be determined together with the static ones. Notice that the density operator e^{-H/k_BT} is the same as the time evolution operator $e^{-iH\tau/\hbar}$ in imaginary time τ if one identifies $\tau = -i\hbar/k_BT$.

This leads to an introduction of an imaginary time direction in the system. When $T \rightarrow 0$ the extra "time" direction diverges as an additional spatial dimension. Furthermore, in the

imaginary time formalism, the temperature T is considered as an inverse time. Thus T can be added as an argument to the free energy density f in the definition of f which follows the quantum homogeneity law to finite temperature [78]

$$f(t,T,B) = b^{-(d+z)} f(tb^{1/\nu}, Bb^{x_B}, Tb^{z}) \qquad (3.19)$$

Comparing Eq. 3.16 and Eq. 3.19, we notice that a QPT in d spatial dimensions is equivalent to the corresponding classical transition in $d_{\text{eff}} = d + z$ spatial dimensions. Notice that the mapping of a QPT to the corresponding classical one in general leads to unusual anisotropic classical systems, and is only valid for the thermodynamics.

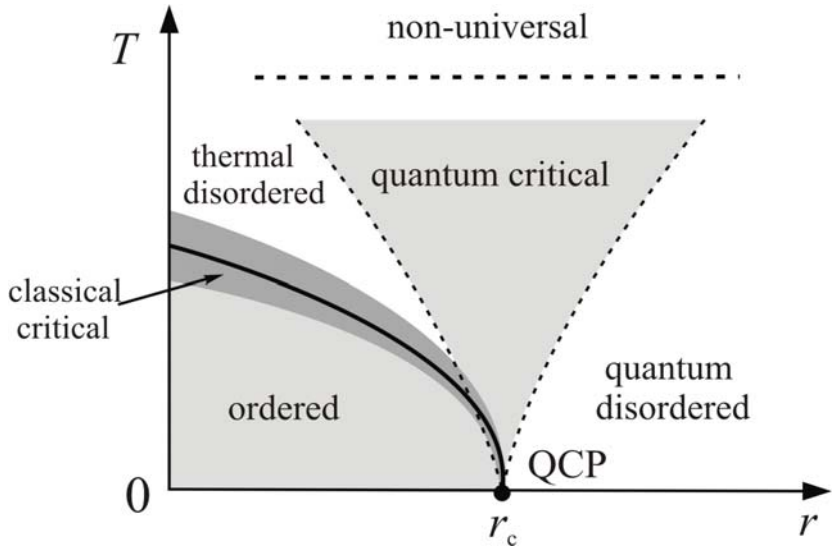

Figure 3.2 Generic phase diagram in the vicinity of a continuous QPT (figure taken from Ref.[9]). Long-range order exists at finite temperatures. The horizontal axis represents the control parameter r used to tune the system through the QPT; the vertical axis is the temperature T. The solid line marks the finite-temperature boundary between the ordered and disordered phases; the end-point of the line located at $r = r_c$ is the QCP. Close to this line, the critical behavior is classical. Dashed lines indicate the boundaries of the quantum critical region where both quantum and classical fluctuations are important; these crossover lines are given by $k_B T \propto | r - r_c |^{\nu z}$; the upper boundary occurs when $k_B T$ exceeds the characteristic microscopic length scales.

At finite temperature, there is a crossover from quantum to classical behavior. If the transition temperature of the system T_C is very small, quantum fluctuations will remain important down to very small $t = |T - T_C|/T_C$, *i.e.* very close to the transition. The behavior at very small but non-zero temperature is determined by a crossover between the quantum and classical behavior. This occurs when the correlation time τ_c reaches $1/k_B T$, which is equivalent to the condition $| t |^{\nu z} < k_B T$.

The full analysis results in a generic phase diagram in the vicinity of a continuous QPT, as shown in Fig. 3.2.

3.2.2. Magnetic quantum phase transition in heavy fermion systems

In heavy fermion systems, the magnetic transitions result from the competition between the Kondo effect and the RKKY interaction (see Section 3.1). Upon varying a control parameter r, like magnetic field, pressure or doping, magnetism is suppressed and the system undergoes a quantum phase transition at the quantum critical point $r = r_c$. Near the QCP, non-Fermi liquid behavior arises. At present, theoretical models, which can give a complete explanation for the origin of the observed NFL behavior, are still lacking. Nevertheless, there are two main scenarios (see for instance Ref.[12]): the *spin-density wave scenario* and the *local-moment scenario* (see Fig. 3.3). These are addressed below.

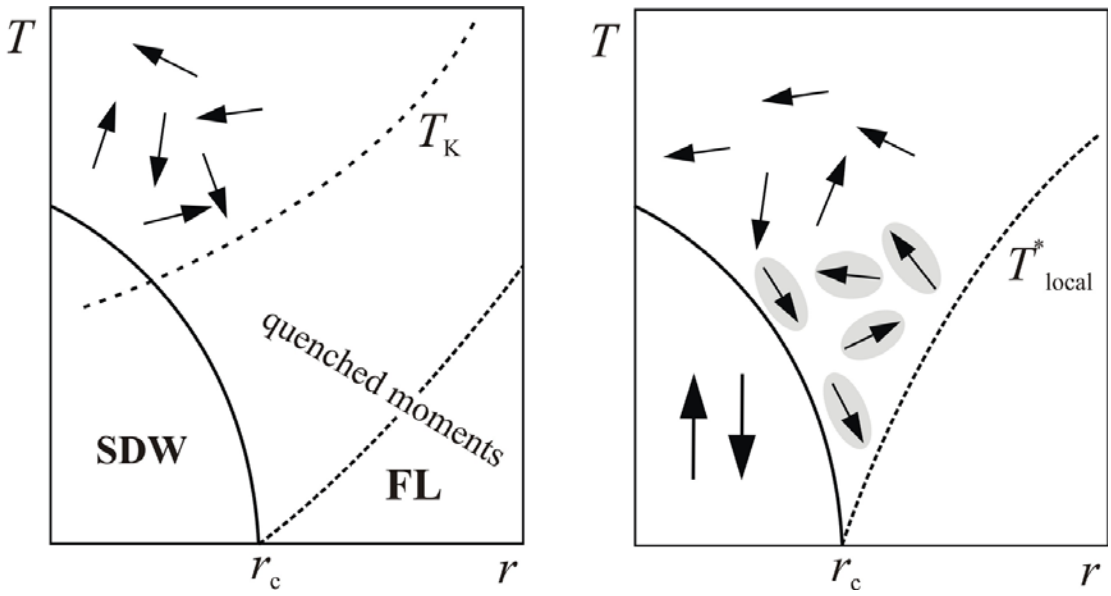

Figure 3.3 Left panel: Spin-density-wave transition in a Fermi liquid. In a Kondo lattice, below a scale T_K, heavy quasi-particles describe well the low-energy excitations of the Fermi liquid. They undergo a magnetic phase transition which has the universality class of a SDW transition. *Right panel*: Breakdown of the Fermi liquid. The Kondo effect, which tries to screen local moments, breaks down near the QCP due to the competition with the RKKY interaction and singular magnetic fluctuations. An effective Kondo temperature T^*_{local} vanishes at the QCP. Picture taken from Ref.[79].

Spin-density wave scenario

In this scenario, the low-energy excitations of the heavy-fermion system below the characteristic Kondo temperature T_K are quasiparticles and their collective excitations. The

Kondo-screened heavy quasiparticles undergo an antiferromagnetic phase transition, which is in the same universality class as the weak-coupling spin-density wave (SDW) transition in the Fermi liquid [80,81].

The SDW scenario for a quantum phase transition at $T = 0$ in itinerant magnets was first studied by Hertz [80] and Moriya [82], and was later revisited by Millis [81]. By studying the effect of non-zero temperature on the QPT, Millis evaluated different regimes of the behaviour of the correlation length, which are identified as the disordered quantum regime, where the Fermi-liquid picture applies, the perturbative classical regime and the classical Gaussian regime. For the latter two regimes, strong departures from the Fermi-liquid behaviour are predicted. In addition, Moriya's self-consistent renormalization (SCR) theory of spin fluctuations for itinerant magnets [82] predicts the same NFL temperature dependences of the thermodynamic properties. The results of the SDW model for the quantum critical regime for an antiferromagnet ($z = 2$) and a (clean) ferromagnet ($z = 3$) are summarized in Table 3.1, for two ($d = 2$) and three ($d = 3$) dimensional systems.

Table 3.1 The temperature dependence of non-Fermi-liquid behavior from the SDW scenario for the specific-heat c/T, the electrical resistivity ρ [82, 83, 84], and the Grüneisen ratio $\Gamma_{\mathrm{r,cr}}$ defined as the ratio of thermal expansion and the specific-heat at the QCP [83] in the low-temperature limit.

	AFM, $z = 2$		FM, $z = 3$	
	$d = 2$	$d = 3$	$d = 2$	$d = 3$
c/T	$-\ln(T/T_0)$	$\gamma - aT^{1/2}$	$T^{-1/3}$	$-\ln(T/T_0)$
ρ	T	$T^{3/2}$	$T^{4/3}$	$T^{5/3}$
$\Gamma_{\mathrm{r,cr}}$	$\dfrac{\log\log(1/T)}{T\log(1/T)}$	$-T^{-1}$	$T^{-2/3}\log(1/T)$	$\dfrac{1}{T^{2/3}\log(1/T)}$

Local-moment scenario

In this scenario, the quasiparticles in the Fermi liquid are bound states in real space, between local moments and conduction electrons. At the QCP the bound states decompose and the effective "Kondo" temperature T^*_{local} vanishes [11,12,73] as shown in the right panel of Fig. 3.3. This suggests a local origin of the singular-Fermi liquid behaviour, as the local moments play an important role in the physics at the QCP.

Precise predictions for the thermal properties in the local QCP model are not available yet. However, very meaningful results have been obtained in the modelling of inelastic neutron-scattering data, taken on systems close to a QCP. Of special interest is the detailed study of $CeCu_{6-x}Au_x$ near the critical concentration $x_c = 0.1$ [73], which revealed a ubiquitous E/T scaling in the dynamical spin susceptibility (here $E = \hbar\omega$ is the excitation energy). E/T scaling provides strong evidence for the emergence of local moments, which are critically correlated in time at the QCP. This is a strong indication that the spin-density wave scenario, which predicts a different scaling form, namely $E/T^{3/2}$, does not capture the essential physics at the antiferromagnetic QCP in $CeCu_{6-x}Au_x$.

3.2.3. Tricritical behavior

Magnetic transitions in metals, from the ordered to the disordered state, are in general continuous (second-order) phase transitions [84]. Additionally, the theory of ferromagnetic (FM) quantum phase transitions developed by Hertz and Millis [80,81] predicts the FM transition to be generically second order. However, experimental studies of QCPs in itinerant ferromagnets have revealed pronounced deviations from the standard second-order behavior. For instance in MnSi [85], UGe_2 [86] and $ZrZn_2$ [14], where the Curie temperature T_C can be tuned to 0 K by applying hydrostatic pressure. Surprisingly, while the magnetic transition at high temperatures is of second order, magnetism vanishes at a first-order QPT. Subsequent, the theoretical studies later suggest that the FM QPT in clean three-dimensional itinerant ferromagnets is always first order due to the correlation effects [87,88].

Further work based on a simple mean-field theory [89] has established the presence of tricritical behavior in itinerant quantum ferromagnets, as shown in Fig. 3.4. If the low Curie temperature (which follows the second-order line in Fig. 3.4) is further decreased by means of pressure tuning, the nature of the transition changes from second order to first order at a tricritical point (TCP). In a small external magnetic field h, the second-order line splits at the TCP leading to surfaces or ‘‘wings’’ of first-order transitions and ends at quantum critical points, see Fig. 3.4. This model successfully describes the QPT for the case of $ZrZn_2$ [14]. However, the first-order nature of QPTs is still an interesting and challenging aspect of the physics of correlated metals.

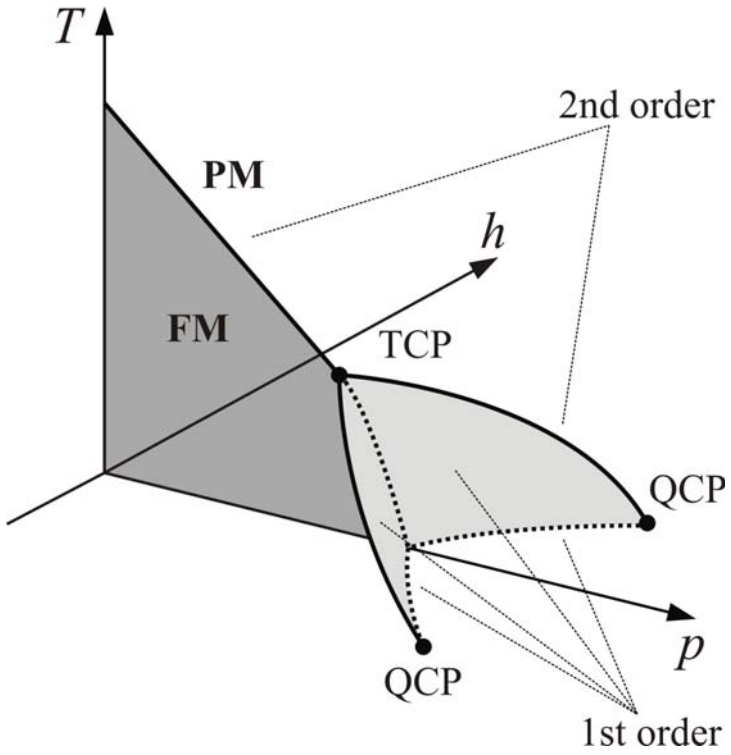

Figure 3.4 Schematic phase diagram of an itinerant ferromagnet, as function of temperature T, pressure p and magnetic field h. FM and PM denote the ferromagnetic (dark shaded) and paramagnetic phases at $h = 0$, respectively. TCP is the tricritical point. The dashed and solid lines represent the first-order and second-order phase transition, respectively. The light shaded area indicates the ‘‘wing’’ surfaces of first-order transitions. Picture taken from Ref.[87].

3.3. Ferromagnetic superconductor

In a superconductor (SC) electrons condense into pairs, the so-called Cooper pairs, which form due to an attractive interaction among electrons at the Fermi surface. The symmetry of Cooper pairs can be defined in terms of the total spin S and the total orbital angular momentum L. A two-electron system can have $S = 0$ or 1 and $L = 0, 1, 2, 3\ldots$ Under the exchange of particles, the total pair-wave function is anti-symmetric which requires a combination of even spatial and odd spin functions or visa versa. This leads to a classification scheme for the symmetry of the Cooper pairs, *i.e.* the spin-singlet state $S = 0$ can be s-wave ($L = 0$) or d-wave ($L = 2$), and the spin-triplet state $S = 1$ is p-wave ($L = 1$) or f-wave ($L = 3$). The spin wave functions with spin-up $\sigma_{\uparrow} = ½$ and spin-down $\sigma_{\downarrow} = -½$ can be represented by:

$$\phi_s = \frac{1}{\sqrt{2}}\left(\left|\uparrow\downarrow\right\rangle - \left|\downarrow\uparrow\right\rangle\right) \qquad (3.20)$$

$$\phi_t = \begin{cases} |\uparrow\uparrow\rangle & (3.21a) \\ \frac{1}{\sqrt{2}}(|\uparrow\downarrow\rangle + |\downarrow\uparrow\rangle) & (3.21b) \\ |\downarrow\downarrow\rangle & (3.21c) \end{cases}$$

where ϕ_s and ϕ_t are the spin-singlet and spin-triplet wave functions, respectively. The two cases described by Eqs. 3.21*a* and 3.21*c* are called *equal-spin pairing* (ESP) state.

In 1957, Bardeen, Cooper and Schrieffer reported a microscopic theory, the well-known BCS theory [32], which successfully describes most superconducting materials. In the BCS theory, the interaction between the electrons of the Cooper pairs is mediated by electron-phonon coupling. The Cooper pairs are of the singlet type with total spin $S = 0$ and angular momentum $L = 0$. Therefore, materials that obey the BCS theory are called *s*-wave or conventional superconductors. However, there are certain classes of superconductors that cannot be understood within the standard BCS theory. These superconductors with condensates made up of Cooper pairs with a lower symmetry (*d*-, *p*-wave...) are called non-*s*-wave or unconventional superconductors. Unconventional superconductivity (or rather superfluidity) was first observed in ^{3}He [90], and later in a wide range of materials, like in heavy fermion compounds [33,34,36,91-97], in high-temperature superconductors (cuprate compounds) [98], and more recently in skutterudites [99]. The mechanism for the formation of Cooper pairs in unconventional superconductors is still one of the major problems in condensed matter physics. There is however much evidence that spin fluctuations rather than phonons provide the superconducting glue.

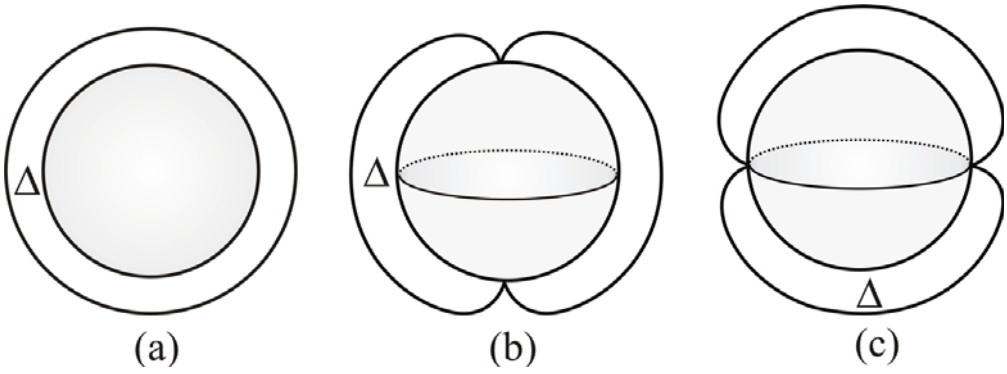

Figure 3.5 Schematic diagram of the energy gap at the Fermi surface of a superconductor. (*a*) The isotropic gap of an *s*-wave superconductor. (*b*) Axial state with point-nodes. The gap vanishes at two opposite points (poles) on the Fermi surface. (*c*) Polar state with line-nodes. The gap vanishes at a line (equator) on the Fermi surface.

The superconducting state is characterized by an order parameter that normally is a gap function $\Delta(\boldsymbol{k})$, which represents the overall magnitude of the energy gap. For conventional superconductors, the superconducting energy gap has the same symmetry as the Fermi surface and is nearly isotropic. For unconventional superconductors, the energy gap has a lower symmetry than the Fermi surface which results in a strong anisotropy and line or point nodes appear in the gap function, which typically indicates a polar or axial state, as shown Fig. 3.5.

By measuring the variation of thermodynamic quantities of superconductors at low temperatures, *e.g.* the specific heat, we can determine the structure of the gap function:

(i) $c \sim e^{-\Delta/T}$, for isotropic gap

(ii) $c \sim (T/\Delta)^3$, for gap with point-nodes

(iii) $c \sim (T/\Delta)^2$, for gap with line-nodes

Among unconventional superconductors, those with superconductivity associated with a magnetic quantum phase transition attract much research interests. By means of changing the non-thermal control parameter, like pressure or magnetic field, magnetism in these systems can be suppressed and tuned to a magnetic quantum critical point (see Section 3.2.2). In the magnetic instability near the QCP, a "dome" of superconductivity emerges and coexists with magnetism. It is believed that in these materials magnetic order and superconductivity are formed by the same electrons and that SC is mediated by magnetic spin fluctuations [35,100]. Fig. 3.6 shows the experimentally determined phase diagrams for systems in which SC coexists with magnetism near a QCP.

Unconventional SC is often observed near a pressure-induced antiferromagnetic QCP, as for example in $CeIn_3$ [33], $CePd_2Si_2$ [33], $CeCu_2Ge_2$ [101], $CeRh_2Si_2$ [102] and $CeRhIn_5$ [103]. Evidence is at hand that in these materials spin fluctuations mediate *d*-wave Cooper pairing which naturally is of the spin-singlet type. Recently, a novel class of superconducting compounds, the so-called ferromagnetic superconductor, has been discovered such as UGe_2 under pressure [34], URhGe at ambient pressure [36], (possibly) UIr under pressure [37] and UCoGe (this work). The idea is that in these compounds, magnetic fluctuations mediate SC by pairing the electrons in triplet states (*p*-wave pairing). Superconductivity coexists with ferromagnetism close to the ferromagnetic QCP. Notice that for the case of URhGe, the quantum tricritical point (TCP) can be approached by

applying of a magnetic field [104]. Since ferromagnetism and SC as a rule exclude each other, the emergence of superconductivity in the vicinity of a FM QCP, came as a big surprise, and has attracted much attention of researchers, both in theory and experiment.

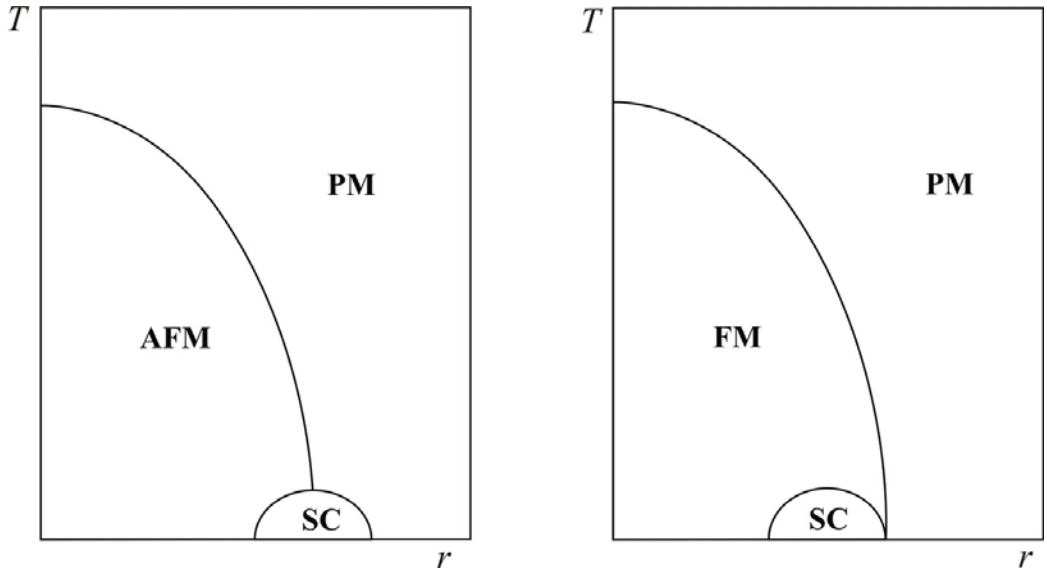

Figure 3.6 Schematic phase diagrams near the QCPs for anti-ferromagnets (*left panel*) and ferromagnets (*right panel*). The horizontal axis represents the non-thermal control parameter *r*, *i.e.* pressure, used to tune the system through the magnetic QPT; the vertical axis is the temperature *T*.

3.3.1. Spin fluctuation and superconductivity

The most popular theory for ferromagnetic superconductivity is due to Fay and Apple [105]. This theory, which is based on the paramagnon exchange mechanism, employs the possibility of an equal-spin pairing SC state in itinerant ferromagnets, where the pairing is mediated by the exchange of longitudinal spin fluctuations. In this model, the superconducting transition temperature is a function of the exchange interaction parameter I, as shown in Fig. 3.7. SC exists in both the paramagnetic ($I < 1$) and the ferromagnetic phase ($I > 1$). For $I = 1$, the QCP is found and $T_S = 0$. Notice that in the FM phase, T_S can be different for the spin-up and spin-down ESP states, which indicates two superconducting phases may exist [105-107].

A more complicated treatment is provided by Roussev and Millis [108]. By means of solving the Eliashberg equations for a 3D-uniaxial system, they found that SC penetrates the FM phase from the PM side, thus T_S is nonzero at the critical point.

However, experiments show the absence of SC in the paramagnetic phase of UGe_2 and UIr.

This is accounted for by the coupling of magnons (FM spin waves) to the longitudinal magnetic susceptibility, which leads to T_S being much higher in the FM phase than in the PM phase [109]. Later work revealed that SC in UGe_2 and URhGe is stimulated by critical fluctuations associated with a magnetic transition between two strongly polarized phases [38,86,110], rather than by fluctuations associated with the FM QCP.

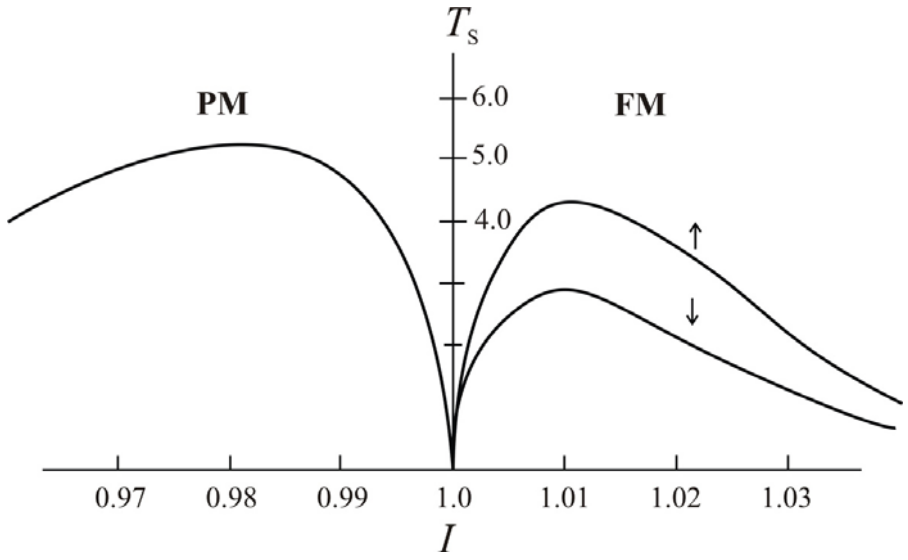

Figure 3.7 Paramagnon exchange mechanism of FM superconductivity. The *p*-state superconducting transition temperature T_S as a function of the exchange interaction parameter I [105]. Here T_S is normalized by the Fermi temperature. The arrows indicate the spin-up (↑) and spin-down (↓) phase.

Clearly, a comprehensive theory that can give a generic, microscopic explanation for the interplay between FM and SC in the small group of ferromagnetic superconductors is still lacking.

3.3.2. Order parameter

A general form of the order parameter and the pairing interaction in a two-band itinerant ferromagnetic superconductor with *orthorhombic* crystal symmetry is given in Refs.[106,111,112]. In this model, it is assumed that ferromagnetic order is uniaxial, with the ordered moment m_0 pointing along the z direction and that spin-orbit interaction is strong. Also, the pairing between electrons in different bands, into Cooper pairs with zero-spin projection is neglected, thus the superconducting state is an ESP state, as given by Eqs. 3.21*a* and 3.21*c*.

Based on a symmetry group analysis the different superconducting basic functions have

been evaluated. The symmetry group $G = M \times U(1)$ consists of the magnetic class M and the group of the gauge transformations $U(1)$.

Any magnetic superconducting state belongs to one of the subgroups of G and is characterized by broken gauge symmetry. In the present case, M is equal to $D_2(C_2^z) = (E, C_2^z, RC_2^x, RC_2^y)$, where R is the time reversal operation. In Ref.[112] Mineev evaluated the subgroups of G which are isomorphic to $D_2(C_2^z)$ and constructed by means of combining its elements, with phase factor $e^{i\pi}$ being an element of the group of $U(1)$. To each of the superconducting magnetic classes corresponds an order parameter. These vector order parameters have the general form:

$$\mathbf{d}(\boldsymbol{R},\boldsymbol{k}) = \eta(\boldsymbol{R})\Psi(\boldsymbol{k}), \tag{3.22}$$

$$\Psi(k) = \hat{x}f_x(k) + \hat{y}f_y(k) + \hat{z}f_z(k) \tag{3.23}$$

where $\hat{x}$, $\hat{y}$, $\hat{z}$ are unit vectors of the spin coordinate system pinned to the crystal axes; $\eta(\boldsymbol{R})$ are the order parameter amplitudes, and $f_{x,y,z}(\boldsymbol{k})$ are odd functions of momentum directions of pairing particles on the Fermi surface. Following Mineev, in the approximation of the strong spin-orbital coupling, the general order parameters for the states have the form [111,112]

$$\Psi^{A_1}(k) = \hat{x}(k_x u_1^{A_1} + ik_y u_2^{A_1}) + \hat{y}(k_y u_3^{A_1} + ik_x u_4^{A_1}) + \hat{z}(k_z u_5^{A_1} + ik_x k_y k_z u_6^{A_1}) \tag{3.24a}$$

$$\Psi^{A_2}(k) = \hat{x}(ik_x u_1^{A_2} + k_y u_2^{A_2}) + \hat{y}(ik_y u_3^{A_2} + k_x u_4^{A_2}) + \hat{z}(ik_z u_5^{A_2} + k_x k_y k_z u_6^{A_2}) \tag{3.24b}$$

$$\Psi^{B_1}(k) = \hat{x}(k_z u_1^{B_1} + ik_x k_y k_z u_2^{B_1}) + \hat{y}(ik_z u_3^{B_1} + k_x k_y k_z u_4^{B_1}) + \hat{z}(k_x u_5^{B_1} + ik_y u_6^{B_1}) \tag{3.24c}$$

$$\Psi^{B_2}(k) = \hat{x}(ik_z u_1^{B_2} + k_x k_y k_z u_2^{B_2}) + \hat{y}(k_z u_3^{B_2} + ik_x k_y k_z u_4^{B_2}) + \hat{z}(ik_x u_5^{B_2} + k_y u_6^{B_2}) \tag{3.24d}$$

where u_1^{A}, … u_6^{B} are real functions of k_x^2, k_y^2, k_z^2; A, B denote the superconducting state with gap function of axial symmetry ($k_x = k_y = 0$) and polar symmetry ($k_z = 0$), respectively, see Fig. 3.5. The order parameter basic functions belong to the different co-representations of the symmetry group of the initial FM state and in general give rise to different critical temperatures. The co-representations for the pair of states A_1, A_2 are equivalent. Here A_1, A_2 present the states in the FM domains with m_0 directed up and down, respectively. The same is true for the states B_1 and B_2.